
Papers

Ångström coefficient as an indicator of the atmospheric aerosol type for a well-mixed atmospheric boundary layer: Part 1: Model development

OCEANOLOGIA, 51 (1), 2009.
pp. 5–38.

© 2009, by Institute of
Oceanology PAS.

KEYWORDS

Ångström coefficient
Effective radius
Atmospheric aerosol mixture
Aerosol composition
Aerosol type

JOLANTA KUŚMIERCZYK-MICHULEC

The Netherlands Organization for Applied Scientific Research,
TNO, The Hague, The Netherlands

On leave from the Institute of Oceanology,
Polish Academy of Sciences, Sopot, Poland;

e-mail: jolanta.kusmierczyk@tno.nl

Received 27 October 2008, revised 9 February 2009, accepted 18 February 2009.

Abstract

The physical and optical properties of an atmospheric aerosol mixture depend on a number of factors. The relative humidity influences the size of hygroscopic particles and the effective radius of an aerosol mixture. In consequence, values of the aerosol extinction, the aerosol optical thickness and the Ångström coefficient are modified. A similar effect is observed when the aerosol composition changes. A higher content of small aerosol particles causes the effective radius of an aerosol mixture to decrease and the Ångström coefficient to increase. Both effects are analysed in this paper. The parameters of the size distribution and the type of components used to represent natural atmospheric aerosol mixtures are based on experimental data. The main components are sea-salts (SSA), anthropogenic salts (WS, e.g. NH_4HSO_4 , NH_4NO_3 , $(\text{NH}_4)_2\text{SO}_4$), organic carbon (OC) and black carbon (BC). The aerosol optical thickness is modelled using the external mixing approach. The influence of relative humidity on the optical and physical properties of the following aerosol mixtures is investigated: (SSA & WS), (SSA & OC), (SSA & BC), (SSA, WS & OC) and (WS, OC & BC). It is demonstrated that the Ångström coefficient can be used as a rough indicator of the aerosol type.

The complete text of the paper is available at <http://www.iopan.gda.pl/oceanologia/>

1. Introduction

The ambient relative humidity changes the optical properties of hygroscopic atmospheric aerosols such as sea-salts. In addition, wetting affects particle sizes and aerosol scattering properties, and ultimately aerosol extinction coefficients and aerosol optical thicknesses. Since aerosols are far from being a single component, the question is how relative humidity influences the optical properties of natural aerosol mixtures, which can contain both soluble and insoluble components.

As the ambient relative humidity (RH) changes, hygroscopic atmospheric aerosols undergo phase transformation, droplet growth, and evaporation. Phase transformation from a solid particle to a saline droplet usually occurs spontaneously when the RH reaches a level called the deliquescence humidity. Its value is specific to the chemical composition of the aerosol particle (e.g. Orr et al. 1958, Tang 1976). To model droplet growth, information about water activity and density as a function of solute concentration is needed. A new technique known as single-particle levitation allows these parameters to be measured properly (e.g. Richardson & Spann 1984, Richardson & Kurtz 1984, Tang & Munkelwitz 1984). The results of a laboratory study of the changes in the optical properties of single-salt and mixed-salt aerosols caused by wetting are presented by Tang (1996, 1997) and Tang & Munkelwitz (1994). It is interesting to apply these results to atmospheric aerosols, which can contain both soluble and insoluble particles.

In the natural environment an increase or a decrease in the aerosol extinction observed at a given wavelength is a sign that measuring conditions have changed. An increase in the aerosol optical thickness or aerosol extinction can be related either to an increase in RH or to a change in the aerosol concentration. Quite often, both factors are present. Optical measurements at one single wavelength will not resolve the question whether the observed change is caused only by the increased humidity or whether the additional aerosol particles have contributed to the measured aerosol extinction or aerosol optical thickness. To be able to retrieve more accurate information about an aerosol mixture, spectral measurements are needed. The more spectral information available, the greater are the chances of getting a more realistic idea of the aerosol composition.

The variation of the extinction coefficient or the aerosol optical thickness with the wavelength can be presented as a power law function with a constant (related to the power factor) known as the Ångström coefficient (Ångström 1929). When the particle size distribution is dominated by small particles, a situation usually associated with pollution, the Ångström coefficients are high; in clear conditions they are usually low. Kuśmierczyk-Michulec & van Eijk (2007) demonstrated that the Ångström coefficient can

be used as a tracer of continental aerosols. It would be interesting to know the extent to which its values change with RH.

The aim of this paper was to investigate the influence of relative humidity on the optical and physical properties of various atmospheric aerosol mixtures. Experimental data on aerosol size distribution, aerosol composition and aerosol optical thickness were used to model aerosol mixtures. Experimental data, including simultaneous optical and chemical measurements, were collected during two cruises on the Baltic Sea in July 1997 and March 1998 as part of the Baltic Sea System Study (BASYS) Atmospheric Load Project (Schultz et al. 1999). The aerosol data relevant to this paper are the measured mass size distributions for sea-salts and anthropogenic salts like ammonium sulphate $((\text{NH}_4)_2\text{SO}_4)$, ammonium nitrate (NH_4NO_3) and ammonium hydrogen sulphate $(\text{NH}_4\text{HSO}_4)$ (Plate 2000), which were used to derive the number size distributions. The relevant optical measurements are the aerosol optical thickness data measured in eight spectral channels (412, 443, 490, 510, 555, 670, 765 and 865 nm, bandwidth 10 nm) with a shadow-band spectrophotometer (Olszewski et al. 1995). These data were presented and extensively described in Kuśmierczyk-Michulec et al. (2001) and Kuśmierczyk-Michulec et al. (2002).

In the first part of this paper a simplified situation is considered. It is assumed that the quantity of aerosol is fixed and that all changes in the optical properties of atmospheric aerosol mixtures can be attributed to the growth of hygroscopic aerosols. The second part will deal with a different scenario: by changing the contribution of aerosol components the influence of aerosol composition on aerosol optical thickness and the Ångström coefficient is analysed. These simulations were done for different RHs covering the range from dry to wet conditions.

This paper presents the theory of the relations between the Ångström coefficient and the composition of atmospheric aerosol mixtures for various RH conditions. The application of these relations will be demonstrated in follow-up papers.

2. Methodology

2.1. Aerosol size distribution and related optical parameters: extinction, aerosol optical thickness and Ångström coefficient

The aerosol size distribution can be represented by the number size distribution $N(r)$, the volume size distribution $V(r)$, or by the mass size distribution $m(r)$. In each case the log-normal function is used. Details are given in e.g. Seinfeld & Pandis (1998).

The aerosol number size distribution for a given aerosol type can be expressed by the following equation, where r is the particle radius, r_n is the median radius and σ is the standard deviation:

$$\frac{dN(r)}{d \ln r} = \frac{N_n}{\sigma\sqrt{2\pi}} \exp \left\{ - \frac{(\ln r - \ln r_n)^2}{2\sigma^2} \right\}. \quad (1)$$

The alternative is the volume size distribution, with the volume median radius r_V and the standard deviation σ :

$$\frac{dV(r)}{d \ln r} = \frac{C_V}{\sigma\sqrt{2\pi}} \exp \left\{ - \frac{(\ln r - \ln r_V)^2}{2\sigma^2} \right\}, \quad (2)$$

where C_V and N_n are particle concentrations for the volume and number size distributions, respectively. The method of conversion from the number size distribution to the volume size distribution is given in e.g. Seinfeld & Pandis (1998). For any log-normal distribution the standard deviation σ in both representations, i.e. the number and volume distributions, is the same.

The volume concentration C_V [$\mu\text{m}^3 \text{cm}^{-3}$] is defined as

$$C_V = \int_{r_{\min}}^{r_{\max}} \frac{dV(r)}{d \ln r} d \ln r. \quad (3)$$

The relation between the volume concentration and the number concentration is given by

$$C_V = \frac{4}{3}\pi N_n \exp\left(\frac{9}{2}\sigma^2\right) r_n^3. \quad (4)$$

The conversion from the volume median radius to the number median radius is given by

$$\ln r_V = \ln r_n + 3\sigma^2. \quad (5)$$

One very useful parameter that can be derived directly from the number size distribution is the effective radius (R_{eff}):

$$R_{\text{eff}} = \frac{\int r^3 \frac{dN(r)}{d \ln r} d \ln r}{\int r^2 \frac{dN(r)}{d \ln r} d \ln r}. \quad (6)$$

It will be demonstrated later that it is advantageous to use the effective radius to characterise aerosol mixtures.

The spectral optical coefficient, called the extinction coefficient $ext(\lambda)$ (in km^{-1}), can be calculated from the number size distribution:

$$ext(\lambda) = \pi \int_{r_{\min}}^{r_{\max}} r^2 Q_{ext} \frac{dN(r)}{d \ln r} d \ln r, \quad (7)$$

or from the volume size distribution:

$$ext(\lambda) = \frac{3}{4} \int_{r_{\min}}^{r_{\max}} \frac{1}{r} Q_{ext} \frac{dV(r)}{d \ln r} d \ln r, \quad (8)$$

where λ is the wavelength, r is the radius and Q_{ext} is the extinction efficiency factor, which is a function of the complex refractive index (Mie 1908). The coefficient Q_{ext} was calculated according to the algorithm of Bohren & Huffman (1983).

The extinction coefficient integrated over the whole column of the atmosphere is a dimensionless parameter and is called the aerosol optical thickness (τ_a):

$$\tau_a(\lambda) = \int_{H_{\min}}^{H_{\max}} ext(\lambda, h) dh \approx \int_{H_{\min}}^{H_{\max}} ext(\lambda) f(h) dh, \quad (9)$$

where $f(h)$ represents the vertical distribution of aerosols, h is the altitude in km, H_{\min} and H_{\max} are respectively the lower and the upper altitude at which a given aerosol type can be found.

The atmosphere can be modelled as the superposition of three layers: the boundary layer (BL), free troposphere and stratosphere. McClatchey et al. (1984) and Hess et al. (1998) assume that within each layer the aerosol composition is constant with height. As a rough estimate, BL is often assumed to have a depth of 2 km.

Variation of the extinction coefficient with wavelength can be presented in the form of a power law function (Ångström 1929):

$$ext(\lambda) = \gamma_c \lambda^{-\alpha}. \quad (10)$$

The same type of relation is also valid for the aerosol optical thickness,

$$\tau_a(\lambda) = \gamma_\tau \lambda^{-\alpha}, \quad (11)$$

where γ_c and γ_τ are constant and α is the Ångström coefficient (also known as the Ångström exponent or Ångström parameter). This parameter is usually determined in the spectral range from 440 nm to 870 nm.

2.2. The main aerosol components, their size distributions and refractive indices

The main aerosol components of natural atmospheric mixtures include sea-salts (SSA), black carbon (BC), organic carbon (OC), and anthropogenic salts like ammonium hydrogen sulphate (NH_4HSO_4), ammonium nitrate (NH_4NO_3) and ammonium sulphate ($(\text{NH}_4)_2\text{SO}_4$), which belong to a large group of water-soluble particles (WS). To model the physical and optical properties of these aerosol components both literature and experimental data were used. The chemical data, collected during two cruises on the Baltic Sea (Schultz et al. 1999), include concentration and size distribution measurements. Concentrations of carbonaceous particles (black carbon and organic carbon) were measured using filters (Rulleau 2000). The aerosol mass size distributions of sea-salts and anthropogenic salts (NH_4HSO_4 , NH_4NO_3 , NH_4HSO_4) were measured using 8-stage BERNER low-pressure impactors (Plate 2000) and then used to derive the number size distributions.

To calculate the extinction coefficient for a given aerosol component both refractive indices and aerosol size distribution parameters are required. All the refractive indices are taken from the literature (see Table 1). Table 2 lists the parameters of the number size distributions. In both cases the following notation is used: the main aerosol components are indicated by capital letters (e.g. SSA, BC, OC, WS), while the different refractive indices or aerosol size distribution parameters for the same aerosol component are denoted by numbers (e.g. SSA1, SSA2).

Table 1. Refractive indices (real and imaginary) of aerosols for the range of wavelengths from 400 to 860 nm

λ [nm]	Black carbon		Organic carbon	WS(1 to 4) ^b	Sea-salts
	BC(1 to 3) ^a	BC4 ^b	OC(1 & 2) ^c		SSA(1 to 6) ^b
400	1.95–0.66i	1.75–0.46i	1.55–0.005i	1.53–0.005i	1.385–0i
488	1.95–0.66i	1.75–0.45i	1.55–0.005i	1.53–0.005i	1.382–0i
515	1.95–0.66i	1.75–0.45i	1.55–0.005i	1.53–0.005i	1.381–0i
550	1.95–0.66i	1.75–0.44i	1.55–0.005i	1.53–0.006i	1.381–0i
633	1.95–0.66i	1.75–0.43i	1.55–0.005i	1.53–0.006i	1.377–0i
694	1.95–0.66i	1.75–0.43i	1.55–0.005i	1.53–0.007i	1.376–0i
860	1.95–0.66i	1.75–0.43i	1.55–0.005i	1.52–0.012i	1.372–0i

^a Ackerman & Toon (1981)

^b McClatchey et al. (1984)

^c Sloane (1983).

Table 2. Parameters of the number size distribution for dry conditions

Aerosol component	Symbol	r_n [μm]	σ	R_{eff} [μm]	α
Black carbon	BC1 ^a	0.0118	0.30	0.0512	1.688
	BC2 ^a	0.02	0.30	0.0534	1.714
	BC3 ^a	0.03	0.30	0.0576	1.733
	BC4 ^b	0.0118	0.30	0.0512	1.648
Organic carbon	OC1 ^a	0.06	0.30	0.0794	3.286
	OC2 ^c	0.03	0.46	0.0726	3.221
Anthropogenic salts:					
NH ₄ HSO ₄	WS1 ^c	0.05	0.46	0.1055	2.461
NH ₄ HSO ₄	WS2 ^d	0.112	0.58	0.3014	0.619
NH ₄ NO ₃	WS3 ^d	0.135	0.58	0.3425	0.449
(NH ₄) ₂ SO ₄	WS4 ^d	0.19	0.68	0.7067	-0.088
Sea-salts (NaCl)					
	SSA1 ^d	0.4	0.51	1.1255	-0.358
	SSA2 ^d	0.4	0.55	1.2512	-0.313
	SSA3 ^d	0.5	0.56	1.6076	-0.214
	SSA4 ^d	0.395	0.57	1.3067	-0.299
	SSA5 ^d	0.32	0.58	1.0893	-0.379
	SSA6 ^d	0.32	0.60	1.1555	-0.355

^a Chylek et al. (1981), Heintzenberg (1982), Berner et al. (1996)

^b McClatchey et al. (1984)

^c Stier et al. (2005)

^d These values are based on the mass size distributions measured over the Baltic Sea (see text for details).

The refractive indices of sea-salts, water-soluble aerosols and black carbon (BC4) are taken from McClatchey et al. (1984). The alternative refractive index for black carbon, indicated by symbols BC (1 to 3), comes from Ackerman & Toon (1981), that for organic carbon from Sloane (1983).

The parameters of the aerosol size distributions come from two sources: the literature, and experiments in the Baltic Sea region. Since the size distribution was not measured for carbonaceous aerosols, some of the most frequently used literature values were assumed. Each set of parameters (r_n , σ) is indicated by a different symbol. Thus, there are four symbols for black carbon: BC1, BC2, BC3 and BC4, and two for organic carbon: OC1 and OC2. The values of the parameters for BC1, BC2, BC3 and OC1 are taken from Chylek et al. (1981), Heintzenberg (1982) and Berner et al. (1996); the values for BC4 come from McClatchey et al. (1984) and those for OC2 from Stier et al. (2005).

The sea-salt aerosol (SSA) number size distributions were derived indirectly from the mass-size distributions of sodium. It is well-known that sodium chloride (NaCl) is the major component of the sea-salt aerosol. Thus, using the formulae for the sodium content in sea salt – SSA [$\mu\text{g m}^{-3}$] = $3.257 \times \text{Na}^+$ [$\mu\text{g m}^{-3}$] – the SSA mass size distribution was calculated from the sodium mass distribution and then converted to the number size distribution. The symbols from SSA1 to SSA6 (see Table 2) correspond to six different sets of parameters (r_n, σ).

The number size distribution parameters for the anthropogenic salts are indicated by four symbols: WS1, WS2, WS3 and WS4. Each one corresponds to a different type of anthropogenic salt, or for the same aerosol type (e.g. WS1 and WS2) to a different set of parameters (r_n, σ). Table 2 gives the details.

The experimental data were presented in Kuśmierczyk-Michulec et al. (2001). Note that for the purpose of the present paper the conversion procedure yielding the number size distributions was repeated. Data were recalculated and a different wetting algorithm was used. Instead of the formulae given by Gong et al. (1997), the more accurate approach suggested by Tang (1996) and Tang & Munkelwitz (1994) was used. Hence, the values of the parameters in Table 2 differ slightly from those in Kuśmierczyk-Michulec et al. (2001).

2.3. Modelling the growth of hygroscopic aerosols

A change in RH alters the size distribution of hygroscopic aerosols like sea-salts (NaCl) and anthropogenic salts, e.g. NH_4NO_3 and $(\text{NH}_4)_2\text{SO}_4$. In this paper it is assumed, as in McClatchey et al. (1984), that black carbon (BC) is not soluble. Despite the fact that about c. 40% of organic carbon (OC) is soluble (S. Rulleau, personal communication; IPCC 2007), for the simplicity and transparency of the calculation, it is assumed that OC is not hygroscopic either.

It would be difficult to estimate the extent to which the latter simplification biases the results. One of the main reasons is that there is still no detailed description of the interactions among organic and inorganic aerosol compounds and water (e.g. Kanakidou et al. 2005). Interest in the hygroscopic properties of OC relevant to atmospheric applications has only recently started to grow, and data are still rather scarce. Hence, considering all the associated uncertainties, neglect of the hygroscopic growth of organic aerosols would seem to be justified.

The increase in particle radius caused by an increase in RH can be found from the equation (e.g. Tang 1996):

$$r_{RH} = r_{dry} \left(\frac{100 \rho_{dry}}{\chi_{RH} \rho_{RH}} \right)^{1/3}, \quad (12)$$

where r_{RH} and r_{dry} are the radii of a wet and dry particle, respectively. Similarly, ρ_{RH} and ρ_{dry} are the respective densities of a wet and dry aerosol. The parameter χ_{RH} is the solute weight percentage (Tang & Munkelwitz 1994) and can be expressed as a function of water activity aw , or simply as a function of RH:

$$\chi_{RH} = \sum_i A_{xi} (aw)^i = \sum_i A_{xi} \left(\frac{RH}{100} \right)^i. \quad (13)$$

Changes in the aerosol density caused by changes in RH are described by:

$$\rho_{RH} = 0.9971 + \sum_i A_{\rho_i} (\chi_{RH})^i. \quad (14)$$

The values of coefficients A_{xi} and A_{ρ_i} for different salts are based on the laboratory work by Tang (1996) and Tang & Munkelwitz (1994).

Two pairs of equations, i.e. (12)–(13) and (1)–(2), were used to calculate the ‘wet’ aerosol size distributions. Variation of σ caused by RH was also included. This effect is not discussed separately, because this paper focuses mainly on the changes in the extinction values caused by relative humidity, i.e. on the indirect result of changes in the aerosol size distributions.

2.4. Modelling the aerosol mixture: external mixing

The optical properties of the aerosol mixture can be represented by the aerosol extinction (see eqs. (7) or (8)) or by the aerosol optical thickness (see eq. (9)). Both parameters can be modelled using the external mixing approach. This means that each aerosol component of a given natural aerosol mixture is represented by a different substance with its own single mode size distribution and single complex index of refraction. The spectral values of the aerosol extinction for a given aerosol component are found from Mie calculations. The aerosol optical thicknesses are obtained as the corresponding weighted averages of the extinction coefficients using the volume percentages. This approach is widely used in aerosol models (e.g. McClatchey et al. 1984, Hess et al. 1998).

Since some aerosol components are hygroscopic, the general equation for the aerosol optical thickness of a natural mixture can be given as

$$\tau_a(\lambda, RH) = \sum_{j=1}^4 C_{V,tot}^j(RH) \times \frac{ext^j(\lambda, RH)}{C_V^j(RH)} = \sum_{j=1}^4 C_{V,tot}^j(RH) \times \psi^j(\lambda, RH), \quad (15)$$

where $j = 1, \dots, 4$ symbolises the aerosol components SSA, WS, OC and BC. The parameter ψ^j indicates the aerosol extinction of the j^{th} component with respect to its volume concentration C_V^j [$\mu\text{m}^3 \text{cm}^{-3}$]. The parameter $C_{V,tot}^j$ [$\mu\text{m}^3 \mu\text{m}^{-2}$] is the total volume of the j^{th} aerosol component in the whole column of the atmosphere. The aerosol components included in a mixture do not exceed four in number. The details concerning the method of calculation are explained in Appendix 1 (page 37).

The aim of this paper is to investigate the changes in the optical properties caused by changes in RH. The optical properties of single aerosol components are assumed to be known, the total aerosol optical thickness at a given wavelength is also known from measurements.

The simulations presented in this paper are valid for a well-mixed boundary layer. In consequence, variations in RH with altitude are not taken into account. The question arises to what extent the above assumption influences the modelling results. In other words, can RH at the measurement altitude represent RH averaged over the whole column? To answer this question radiosonde measurements made during the BASYS experiment were used. For each single radiosonde launching, the column integrated value $\langle \text{RH} \rangle_{\text{col}}$ was calculated and compared to the value representing the surface measurements RH_{meas} . Analysis of the data from both summer and winter experiments revealed that the mean value of the absolute difference $|\text{RH}_{\text{meas}} - \langle \text{RH} \rangle_{\text{col}}|$ was about 15% (i.e. $15\% \pm 10\%$).

The aerosol optical thickness represents the column integrated extinction. Hence, it would be difficult to estimate the significance of the above simplification in a more accurate way without knowing a priori the vertical RH profile and the vertical aerosol profile, or alternatively, the changes in the aerosol extinction with altitude.

3. Influence of relative humidity on the optical properties of aerosol mixtures containing a fixed number of particles

This section analyses the case when the number of aerosol particles is fixed and the only variable parameter responsible for changes in the aerosol optical thickness is the relative humidity (RH).

3.1. Pure salts: SSA and WS

In a pure marine environment the observed aerosol types are sea-salts. However, such an ideal situation exists only in a remote area, over the open ocean. Everywhere else there is usually some admixture of anthropogenic salts. Both types of salts are hygroscopic. An increase or decrease in RH causes changes in the size, volume and density of the particles, and

eventually in the aerosol optical thickness. The only parameter independent of RH is the number of particles.

Figure 1a illustrates changes in the aerosol extinction of sea-salts, $ext^{SSA}(\lambda, RH)$. The simulations are presented for three aerosol types – SSA1, SSA3 and SSA5 – and two wavelengths – 412 and 865 nm. In all cases the same number of particles is assumed. Regardless of the size distribution, the extinction increases significantly, especially when $RH > 80\%$. An increase

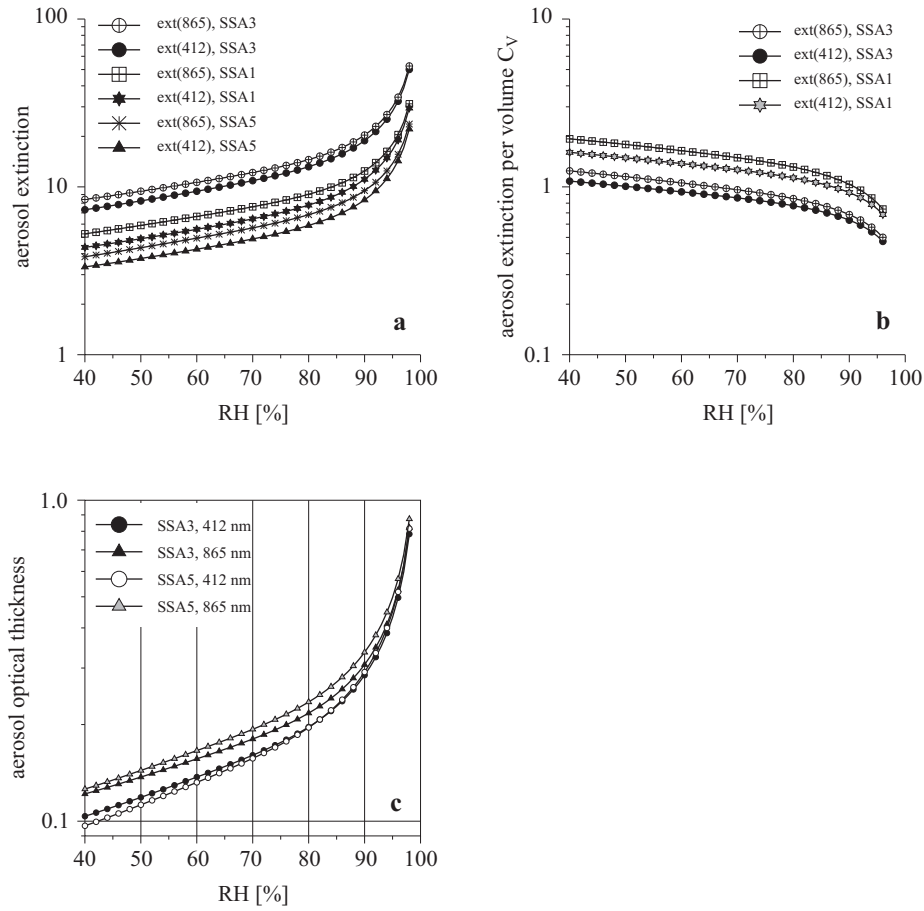


Figure 1. Influence of relative humidity (RH) on aerosol optical properties at two wavelengths: 412 nm and 865 nm. a) Sea-salt extinction, ext^{SSA} , as a function of RH. Three types of sea-salts are compared: SSA1, SSA3 and SSA5. b) Sea-salt extinction with respect to volume: $ext^{SSA}(\lambda, RH)/C_V^{SSA}(RH)$. Calculations are presented for two types of salts: SSA1 and SSA3. c) Increase in aerosol optical thickness due to increasing RH. The number of particles was estimated for the conditions at which the ambient $RH = 80\%$ and $\tau_a(555) = 0.2$. The simulation results are presented for two types of salts: SSA3 and SSA5

in RH leads to a rise in C_V , which affects the resultant ratio (here index j is replaced by the symbol SSA, see eq. (15)):

$$\psi^{SSA}(\lambda, RH) = ext^{SSA}(\lambda, RH)/C_V^{SSA}(RH). \quad (16)$$

Figure 1b presents values of the sea-salt aerosol extinction with respect to volume concentration C_V . Though shown for only two types of salts, they illustrate the general pattern, also observed for other size distributions.

Figure 1c illustrates modifications of the aerosol optical thickness, which at the moment of measurement at $RH = 80\%$ and $\lambda = 555$ nm is equal to 0.2, i.e. $\tau_a(555, RH_{80}) = 0.2$. These initial conditions are used to estimate the number of particles, and then to simulate the results for different RH following the method described in Appendix 1. The simulations are repeated for the six aerosol number size distributions SSA (1 to 6) listed in Table 2.

Wetting causes the aerosol optical thickness τ_a to increase significantly, especially when $RH > 90\%$; at $RH = 98\%$ this may be up to 6 times its value at $RH = 80\%$. This effect is observed at both wavelengths, but for higher RH, the increase in the aerosol optical thickness is more evident at 412 nm than at 865 nm. This different behaviour is also demonstrated in Figure 1b. As a consequence of such a non-uniform increase, the Ångström coefficient also becomes a function of RH.

Figure 2a shows the Ångström coefficient as a function of RH. Each of the 6 curves represents a different size distribution, indicated by the symbols SSA1 to 6. The increase in RH gives rise to changes in the Ångström

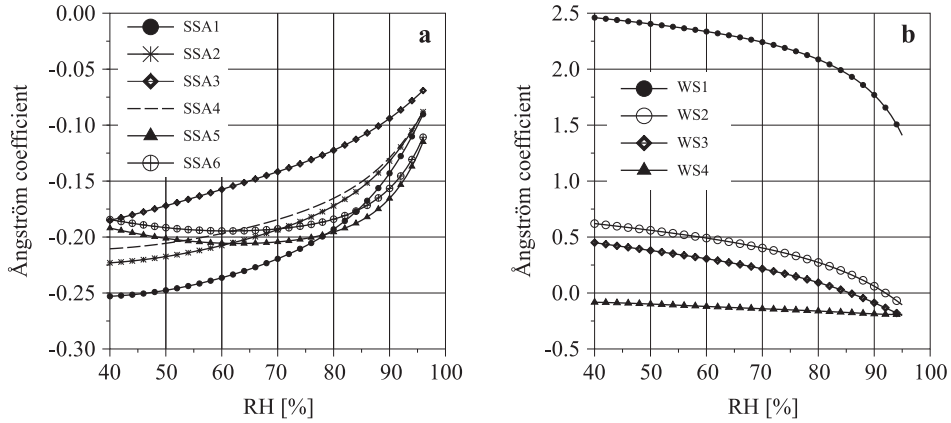


Figure 2. Changes in the Ångström coefficient are the result of wetting and increase in aerosol size. The Ångström coefficient as a function of relative humidity (RH) for a) six different sea-salt distributions, b) four different anthropogenic salt distributions. The symbols are explained in Table 2 (page 11)

coefficients, which depend on the aerosol size distribution. Unlike curves SSA5 and SSA6, curves SSA1, SSA2, SSA3 and SSA4 clearly increase with RH. It will be noticed that the upper threshold value does not exceed -0.05 . Since there are some similarities between the curves, it suffices to analyse three of them rather than all six – SSA1, SSA5 and SSA3, representing the lower, middle and upper curves, respectively. The lower curve (SSA1) corresponds to the narrowest of all the size distributions (standard deviation for dry conditions $\sigma = 0.51$), the middle curve (SSA5) represents the size distribution with a much smaller dry median radius than the other salts, and the upper one (SSA3) represents the size distribution with the largest dry median radius.

The same type of simulation as for sea-salts was repeated for the anthropogenic salts. Figure 2b shows the Ångström coefficient as a function of RH for two size distributions of NH_4HSO_4 , represented by symbols WS1 and WS2, one distribution of NH_4NO_3 (WS3) and one distribution of $(\text{NH}_4)_2\text{SO}_4$ (WS4). The influence of RH on the Ångström coefficient is more significant than in the case of sea-salts. Interestingly, the curves representing salts WS2, WS3 and WS4 are clearly separated from the WS1 curve. The first group of curves is located in the bottom part of the graph and does not exceed the threshold value of 0.6. In contrast, curve WS1 lies in the upper part of the graph with a threshold value almost four times greater than that of the other salts. This effect can be explained by the significant difference in the size distributions. The WS1 size distribution is narrower and has a dry median radius half that of the other salts. In all cases the same behaviour is observed: the drier the aerosol, the larger the Ångström coefficient. Wetter conditions cause anthropogenic salt particles to grow and the Ångström coefficient to decrease.

3.2. Two-component aerosol mixtures – SSA & WS, SSA & OC and SSA & BC

In the marine environment, the aerosol type usually observed is a mixture of sea-salts and anthropogenic salts. Such a natural mixture may also contain some organic carbon or black carbon. These latter two aerosol components are assumed to be insoluble. What is the effect of RH in this case?

Figure 3 shows the variation in the Ångström coefficient for four different mixtures consisting of SSA3 and NH_4HSO_4 WS1 (Figure 3a) and WS2 (Figure 3b). Each curve represents a mixture with a different percentage of anthropogenic salt (5 – 20%). Both plots show that the addition of a small amount of anthropogenic salt causes the optical properties of the aerosol mixture to differ significantly from those of the pure sea salt; the Ångström

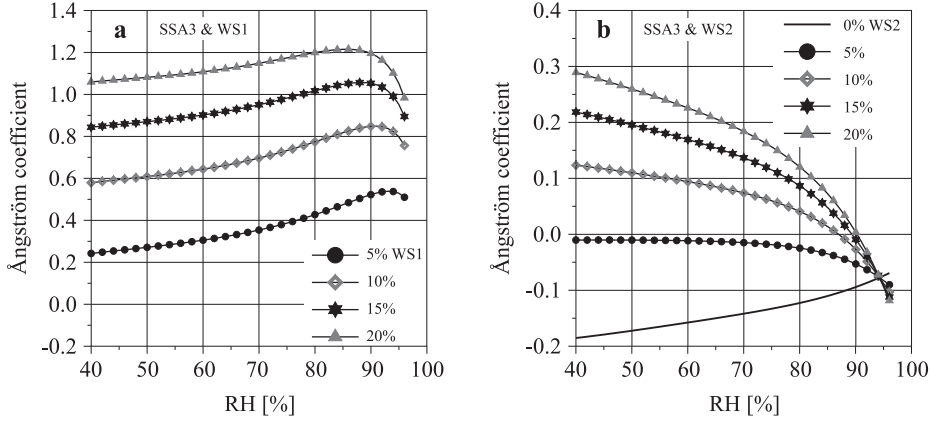


Figure 3. Changes in the Ångström coefficient caused by an increase in relative humidity (RH) for four different mixtures consisting of SSA3 and ammonium hydrogen sulphate WS1 (a) and WS2 (b). Each curve represents a mixture with a different percentage of anthropogenic salt (5 – 20%). For comparison, the curve representing the pure sea-salt SSA3 is also plotted (b)

coefficient is much higher than that of the pure sea-salt components. Both graphs also show that the same Ångström coefficient value may correspond to a different percentage of WS depending on its initial size distribution parameters, e.g. $\alpha = 0.265$ at $\text{RH} = 48\%$ may represent either a mixture of sea-salts and 20% WS2 or a mixture of sea-salts and 5% WS1.

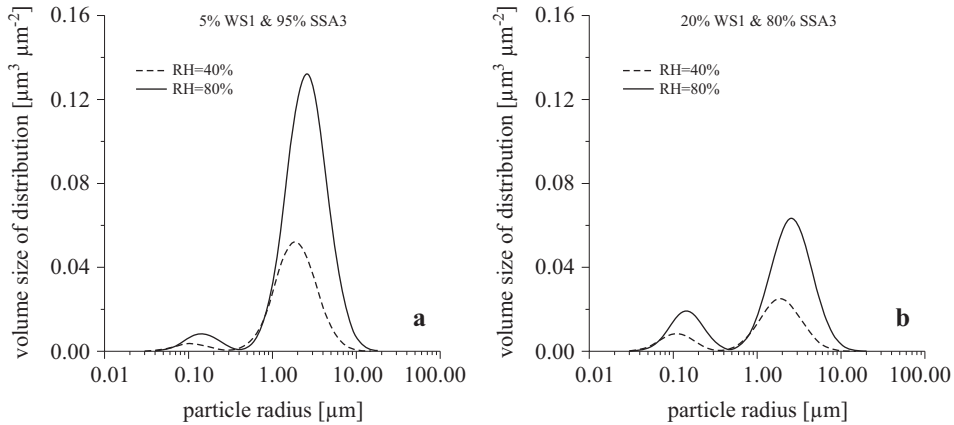


Figure 4. Changes in the size distribution of an aerosol mixture consisting of SSA3 and WS1, demonstrated for relative humidities (RH): $\text{RH} = 40\%$ and $\text{RH} = 80\%$. The smaller peak on the left represents the contribution from anthropogenic salt; the higher one on the right represents sea-salt. The simulations were done for two mixtures: (a) 95% SSA3 + 5% WS1 and (b) 80% SSA3 + 20% WS1

Figures 4a and 4b illustrate the changes in the size distribution of the aerosol mixture. A 100% increase in RH causes the volume concentrations of both fine (WS1) and coarse particles (SSA3) to almost double, i.e. $C_V^{WS1}(RH_{80})/C_V^{WS1}(RH_{40}) \approx 2.3$, and $C_V^{SSA3}(RH_{80})/C_V^{SSA3}(RH_{40}) \approx 2.5$. On the other hand, for the same RH, a similar effect is observed when the percentage of one aerosol compound in the aerosol mixture increases. The contribution of the fine mode increases by 15%, i.e. from 5 to 20%, and the ratio between the volume concentration of fine particles (WS1) is almost doubled: $C^{WS1, 20\%}/C^{WS1, 5\%} \approx 2.3$.

RH modifies the optical properties not only of hygroscopic aerosol mixtures but also of mixtures containing certain amounts of non-hygroscopic aerosols, such as organic carbon or black carbon. Figure 5a presents the Ångström coefficients for a mixture of SSA3 and OC1. The different percentage of OC1 is indicated by different symbols. Similar calculations were repeated for OC2. For both types of organic carbon the same percentage produces a similar result. To illustrate this effect, Figure 5b shows the difference between the Ångström coefficients for both mixtures containing OC1 and OC2: α increases with increasing OC and decreases with increasing RH.

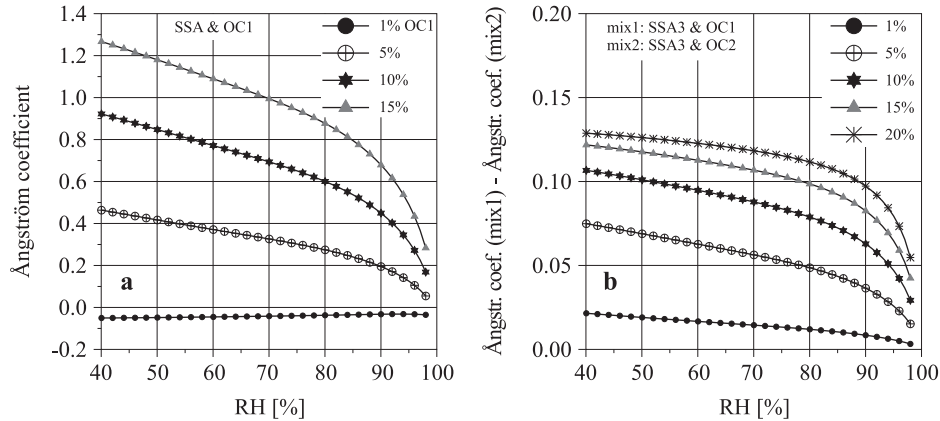


Figure 5. The Ångström coefficient of aerosol mixtures as a function of relative humidity (RH). a) Mixture of SSA3 and OC1. b) Difference between the Ångström coefficients for two mixtures: SSA3 & OC1 and SSA3 & OC2. The percentage contribution varies from 1% to 20%

The black carbon content behaves in a similar way. Figure 6 shows that a small amount of black carbon has the same effect as a much larger amount of OC or WS. For example $\alpha = 0.1$ at $RH = 80\%$ may represent

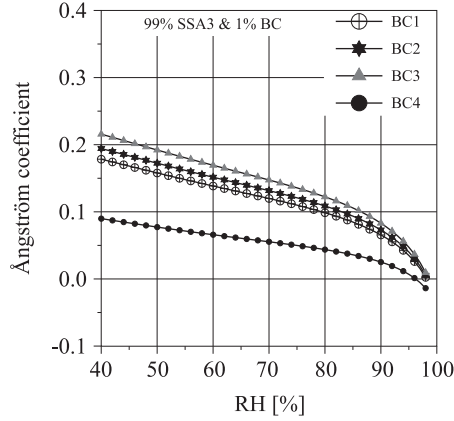


Figure 6. Variations in the Ångström coefficient with relative humidity (RH). The simulations were done for four types of black carbon: BC1, BC2, BC3 and BC4 (see Table 2 for explanations). The percentage contribution of black carbon is assumed to be 1%

either a mixture of sea-salts with 1% BC1 (Figure 6) or a mixture of sea-salts and 15% WS2 (Figure 3b). Similarly, $\alpha = 0.6$ at $\text{RH} = 80\%$ may stand for a mixture of sea-salts and a content of 5% BC1 or 10% OC1 (Figure 5a).

Changes in the value of the Ångström coefficient can be related to changes in the effective radius of a mixture. A greater content of small aerosol particles causes the effective radius to decrease and the Ångström coefficient to increase. An increase in RH influences the size of hygroscopic

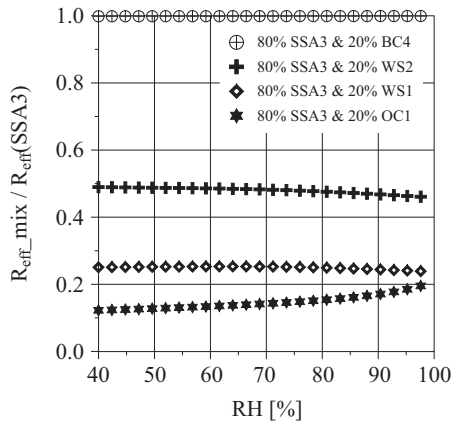


Figure 7. Ratio between the effective radius (R_{eff}) of pure SSA3 and a mixture consisting of 80% SSA3 and 20% of another aerosol component. The different symbols indicate different aerosol components

particles and, consequently, the effective radius of an aerosol mixture. Figure 7 shows the ratio between the effective radius of pure sea-salts and a mixture. Particles of WS1 are much smaller than those of WS2; therefore, the effective radius of the second mixture (SSA3 & WS2) is larger than that of the first one (SSA3 & WS1). Both mixtures are hygroscopic and RH has a similar influence on the effective radius of a mixture and pure sea-salts. Therefore, the ratio between both parameters will be nearly constant. The situation is different in the case of OC, which is insoluble. OC particles are small, and the effective radius of a mixture will be much smaller than that of pure sea-salts. On the other hand, as RH increases, so does the radius of sea-salt particles; hence the slight increase in the effective radius with RH. Black carbon particles behave differently. On the one hand, these are so small that they do not change the effective radius of a mixture, but on the other, even a small admixture of black carbon particles will alter the value of α . This can be explained by the strong absorbing properties of black carbon. These changes will be discussed in detail in the next section.

4. Influence of aerosol composition on the optical properties of an aerosol mixture for a given relative humidity

The previous section discussed the situation where all changes in the aerosol optical properties were caused only by wetting. For that purpose the number of particles was fixed: for example, in some simulations it was assumed that the number of particles is such that the measured aerosol optical thickness at 555 nm and RH = 80% is 0.2. If the amount of aerosol is fixed, all the changes in the aerosol optical properties can be attributed to the growth of hygroscopic aerosols, which are the result of the increase in RH.

This section focuses on the situation in which all changes in aerosol optical properties for a given RH are caused only by a modified aerosol composition. The simulations are done for RHs from 40 to 96%.

4.1. Two-component aerosol mixtures – SSA & WS and SSA & OC

Let us assume that the aerosol mixture is composed of sea-salts SSA and anthropogenic salts WS. Changes in the content of the latter component $C_{V,tot}^{WS}$ cause the resultant aerosol optical thickness (eq. (15)) to change as well. Figure 8a illustrates the situation where the anthropogenic salt WS1 gradually replaces the amount of sea-salt. Since anthropogenic salt particles are much smaller than sea-salt particles, the number of particles in this particular mixture effectively increases and the resultant volume decreases. As a result the Ångström coefficient increases. Figure 8b illustrates

a similar situation but for a different salt – WS2. In both cases the lowest values correspond to the pure sea-salts, the highest ones to the pure anthropogenic salts.

Figure 8b shows that for an aerosol component like WS2, the maximum Ångström coefficient does not exceed 0.6 for $RH = 40\%$ and 0.3 for $RH = 80\%$. For the same RHs but for a different aerosol component WS1 (Figure 8a), the maximum Ångström coefficients are several times larger; 2.4 and 2, respectively.

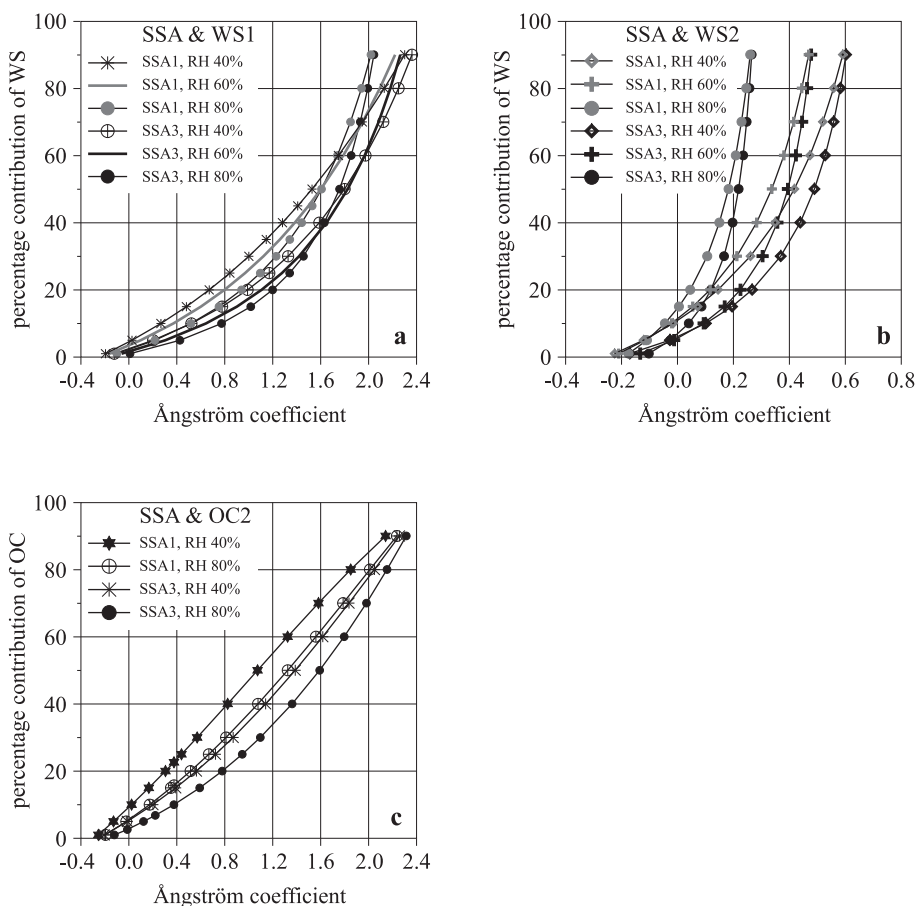


Figure 8. Changes in the Ångström coefficient due to changes in the composition of the aerosol mixture. The lowest values correspond to pure sea-salts. All simulations were done for two types of sea-salt – SSA1 and SSA3. a) Mixture of sea-salts and WS1. b) Mixture of sea-salts and WS2. c) Mixture of sea-salts and OC1. Figures a) and b) present simulations for three relative humidities (RH): $RH = 40\%$, $RH = 60\%$ and $RH = 80\%$, and Figure c) shows simulations for two RHs: $RH = 40\%$ and $RH = 80\%$

Figure 8c shows the effect of replacing the hygroscopic salts WS in this two-component mixture with insoluble organic carbon OC1. Raising the OC content to 20% produces a similar result as for WS1 particles (see Figure 8b). The Ångström coefficient gradually increases from the values characteristic of a given pure sea-salt type to values between 0.6 and 1.2, depending on the RH. A further increase in the OC content causes the Ångström coefficient to increase faster, reaching a maximum of around 3. These interrelations can be explained in terms of changes in the effective radius of a mixture.

Figure 9 illustrates the transition from pure sea-salts to pure OC or WS. The lower the RH, the drier the sea-salt particles and the smaller the effective radius. These changes mostly influence the scattering properties of

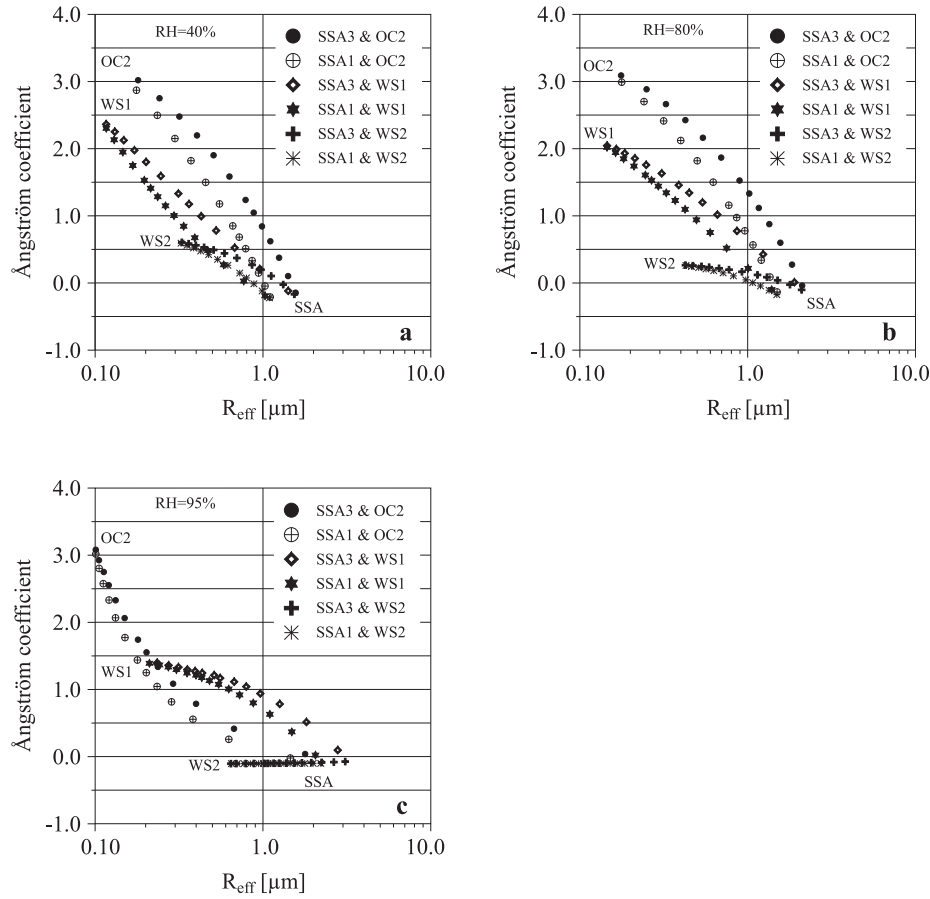


Figure 9. The same mixtures as in Figures 8(a)–(c). The Ångström coefficient is plotted as a function of the effective radius (R_{eff}) of a given mixture. Simulations are presented for relative humidities (RH): a) RH = 40%, b) RH = 80%, c) RH = 95%

the aerosol mixture, but absorbing properties also contribute to the spectral values of the aerosol optical thickness, and eventually to the Ångström coefficient. Therefore, as Figure 9 shows, there is no unique relationship between R_{eff} and the Ångström coefficient, unless the components of the aerosol mixture are known. For an aerosol mixture of two components, e.g. sea-salts and OC or sea-salts and WS, the aerosol optical thickness for a given RH is defined by equation (15). For this kind of mixture, the changes in the Ångström coefficient are given by

$$\alpha_{mix}(RH) = \alpha^{SSA}(RH) - \frac{1}{\ln\left(\frac{\lambda_1}{\lambda_2}\right)} \left\{ \ln \left[1 + \frac{y^{ad}}{\xi} \left(\frac{\lambda_1}{\lambda_2}\right)^{-\alpha^{mix}} \right] - \ln \left(1 + \frac{y^{ad}}{\xi} \right) \right\}, \quad (17)$$

where $\lambda_1 = 412$ nm, $\lambda_2 = 865$ nm and $\xi = \frac{100-x1}{x1}$. Parameter $x1$ represents the percentage contribution of a second aerosol component added to a mixture and is a number between 1 and 100. If $x1$ is equal to 0, then the aerosol mixture consists of pure sea-salts.

Parameters y^{ad} and α^{mix} for a mixture of SSA and WS are defined as follows:

$$y^{ad} = \frac{\psi^{WS}(\lambda_2, RH)}{\psi^{SSA}(\lambda_2, RH)}, \quad (18)$$

$$\alpha^{mix} = \alpha^{WS} - \alpha^{SSA}. \quad (19)$$

The corresponding parameters for a mixture of SSA and OC are given by:

$$y^{ad} = \frac{\psi^{OC}(\lambda_2)}{\psi^{SSA}(\lambda_2, RH)}, \quad (20)$$

$$\alpha^{mix} = \alpha^{OC} - \alpha^{SSA}. \quad (21)$$

A consequence of equations (15) and (11), equation (17) describes the transition from one aerosol type to the other and the related change in the value of the Ångström coefficient.

4.2. Three-component aerosol mixtures: SSA, WS & OC

If a mixture consists of more than two aerosol components, it becomes more difficult to investigate all the changes affecting the value of the

Ångström coefficient. Consider a mixture of SSA and two other components like WS and OC. To simplify this complex situation we shall assume that the mutual relations between WS and OC (WS:OC) are limited to two cases: 1:1 and 2:1. This means that in the first situation the amounts of WS and OC are equal, and in the second case, there is one part OC to two parts WS.

Figure 10 illustrates the changes in the Ångström coefficient due to changes in the composition of the aerosol mixture when $RH = 60\%$. Regardless of the aerosol type, the mixture with the greater OC content has the larger Ångström coefficient. The aerosol mixture composed of sea-salt and WS and OC in equal proportions (WS:OC=1:1) has a much higher Ångström coefficient than the same aerosol components mixed in a different ratio, i.e. WS:OC=2:1. The highest values are generated by an aerosol mixture consisting of fine particles WS1 and OC mixed in equal proportions, the lowest ones by a mixture of OC and WS4 mixed in the ratio 1:2. This becomes clear when the effective radii of these different mixtures are compared. Figure 11 shows the changes in the Ångström coefficient values versus the effective radius. As in the case of the two-component mixture (see Figure 9) there is no unique correspondence between R_{eff} and the Ångström coefficient. The drier conditions (Figure 11a) mean that the aerosol particles representing a mixture are smaller and the Ångström coefficients are slightly higher than for wetter conditions (Figure 11b).

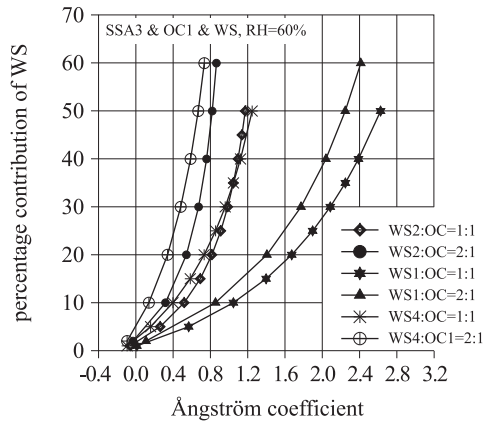


Figure 10. Changes in the Ångström coefficient due to changes in the composition of the aerosol mixture. All simulations were done for relative humidity $RH = 60\%$, one type of sea-salt (SSA1), one type of organic carbon (OC1) and three types of WS (WS1, WS2 and WS4). All types of WS are mixed in different proportions with OC1: WS2:OC1=1:1 and WS2:OC1=2:1

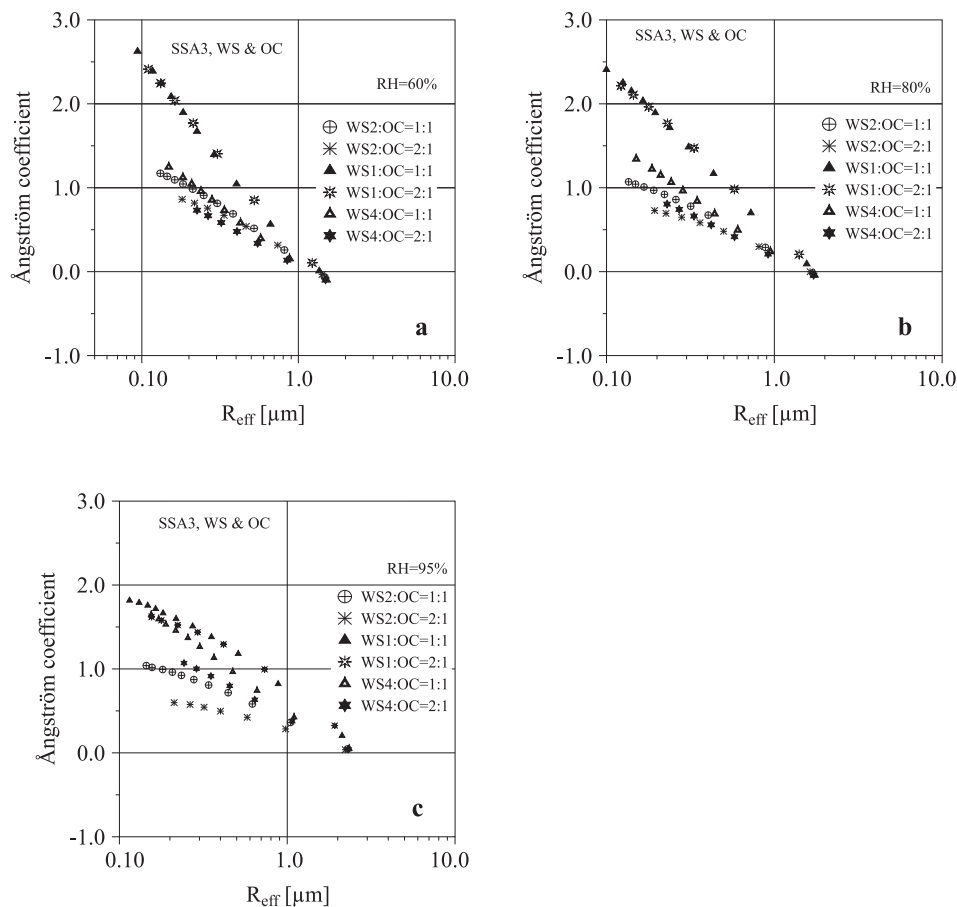


Figure 11. Changes in the Ångström coefficient with effective radius (R_{eff}) for the same mixtures as presented in Figure 10, for relative humidities (RH): RH = 60% (Figure 11a), RH = 80% (Figure 11b) and RH = 95% (Figure 11c)

The mathematical expression describing the changes in the Ångström coefficient of an aerosol mixture composed of sea-salts and two other components like WS and OC is discussed in Appendix 2 (page 38).

4.3. Three-component aerosol mixtures: WS, OC & BC

Aerosol mixtures composed of SSA with certain amounts of WS, OC or BC can represent the typical situation observed over coastal waters or inland seas like the Baltic or Mediterranean. In such a case the continental/industrial aerosol (e.g. BC, OC, WS) is easily transported by air masses and mixed with the marine aerosols (SSA).

The situation at a land station is different. In this case, the aerosol will also be a mixture, but its components will depend on the type of aerosol emitted by nearby sources, e.g. factories. To some extent we can represent the terrestrial mixture by three main aerosol components: WS, OC and BC. Figure 12 shows the Ångström coefficients for aerosol mixtures consisting of these three components; the simulations were done for three RHs: 40, 60 and 80%. Initially, the mixture consisted only of WS and OC. Gradually, the percentage of BC increased and replaced WS and OC (WS:OC=1:1). For example, when there was 10% BC, the contributions of WS and OC were 45% each. The simulations were done for two types of black carbon – BC3 and BC4 – and two types of anthropogenic salts – WS2 and WS1.

In both cases (see Figures 12a and 12b), the addition of the BC component does not change the effective radius of the aerosol mixture. Nevertheless, the Ångström coefficient is modified. The reason is that BC has strong absorbing properties which influence the final aerosol extinction/optical thickness and in consequence also the Ångström coefficient. Figure 12a presents a situation that seems quite obvious: an elevated BC content causes α to increase. Figure 12b, in contrast, illustrates a rather unexpected situation. In this case it turns out that replacing WS1 and OC1 by BC causes an effect opposite to the one observed in Figure 12a. This is

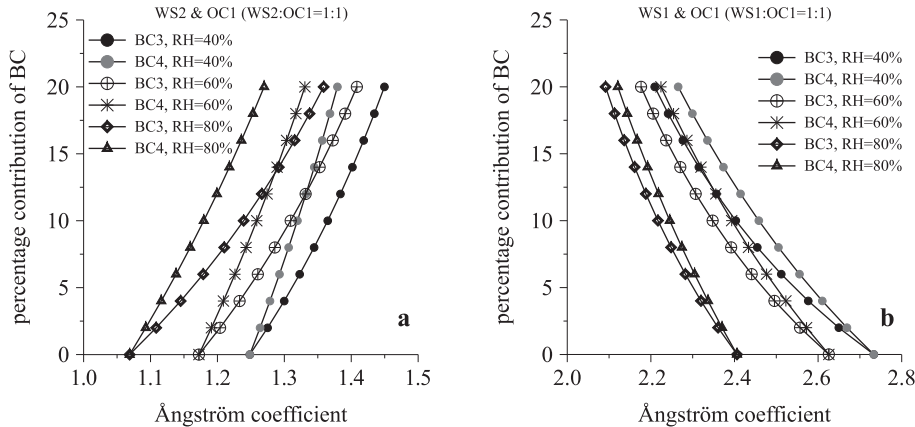


Figure 12. Ångström coefficients for aerosol mixtures consisting of WS, OC and BC. The simulations were done for relative humidities (RH): RH = 40, RH = 60 and RH = 80%. Initially the mixture was composed only of WS and OC. Gradually, the percentage contribution of BC increased and replaced WS and OC (WS:OC=1:1): for example, when the contribution of BC was 10%, those of WS and OC were 45% each. The simulations were done for two types of BC: BC3 and BC4 and two types of WS: a) WS2 and b) WS1

because the contribution from scattering at WS1 and OC1 is much stronger than that due to absorbance by BC. Thus, replacing WS1 and OC1 with BC causes the Ångström coefficient to decrease slightly.

4.4. Why are spectral measurements so important?

Measurements at one single wavelength will not supply accurate information about the aerosol mixture. Figure 13 shows that one single measurement of the aerosol optical thickness at one wavelength, e.g. $\lambda = 555$ nm, will not provide unique information about an aerosol type. The condition that $\tau_a(555) = 0.2$ at RH = 80% was satisfied by four different mixtures: SSA3 & WS2, SSA3 & WS1, SSA3 & OC and SSA3 & BC4. Moreover, in all cases the percentage of sea-salts was 80 and 20% of another component. The main difference was in the number concentration of the second aerosol component. For example, the number of WS1 particles needed to satisfy the conditions was 18 times higher than the number of WS2 particles. OC particles are much smaller than WS1 and WS2, thus a greater amount of them are needed; in fact, there are 111 times more of them than WS2. For BC4, 6757 times more of them than WS2 are needed.

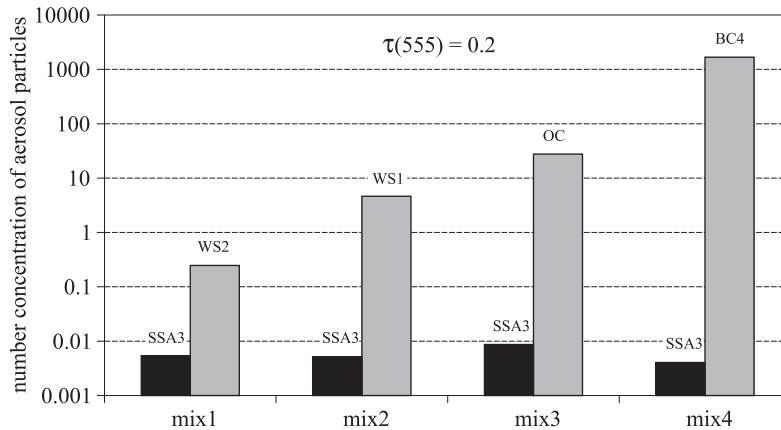


Figure 13. Four different aerosol mixtures consisting of 80% SSA3 and 20% of another aerosol component, e.g. WS2, WS1, OC1 or BC4. In each case the measured aerosol optical thickness (τ_a) at 555 nm and relative humidity RH = 80% is 0.2, i.e. $\tau_a(555) = 0.2$. Different mixtures can satisfy this condition, but the main difference is in the number concentration of aerosol particles of the second aerosol component

If spectral measurements were available, they would provide an additional parameter, the Ångström coefficient. This would help to distinguish

the four mixtures in this example. In a real situation the Ångström coefficient can indicate the probable aerosol type, which would also be useful information.

5. Classification of aerosol mixtures in terms of Ångström coefficients

With changing atmospheric conditions and rising or falling RH, the measured aerosol optical thickness/extinction likewise changes. The effective radius of a mixture alters, and so does the Ångström coefficient. The question is whether these changes can be quantified.

Figure 14 shows how the effective radius (Figure 14a) and the Ångström coefficients (Figure 14b) will change as a result of the transition from drier to wetter conditions and vice versa. The simulations were done for various mixtures, but the difference is always calculated for the same type of mixtures. Figure 14a illustrates the effect of the transition to drier conditions (i.e. from RH = 80% to RH = 60%) and to wetter ones (i.e. from RH = 80% to RH = 95%). In both cases the effective radii change, and the differences are the most significant for Ångström coefficients ≤ 0.5 . Figure 14b presents a similar effect but with respect to the Ångström coefficients. The maximum absolute difference between the Ångström coefficients estimated at RH = 80% and RH = 60% does not exceed 0.2. The transition from RH = 80% to RH = 95% causes more significant changes: for $\alpha < 1.75$, the maximum absolute difference is ≤ 0.3 , but for $\alpha \geq 1.75$ this difference can reach a value of 0.5.

The results presented in Figure 14a suggest that the Ångström coefficient could be regarded as an indicator of atmospheric aerosol type. As already demonstrated in the previous sections, there is a general relationship between R_{eff} and the Ångström coefficient. Higher values of R_{eff} usually correspond to lower values of the Ångström coefficient, and vice versa. Each particle size range is characteristic of a given aerosol mixture. Thus, the observed tendency suggests that the Ångström coefficient could be used to define ‘domains’, indicating possible aerosol mixtures and then aerosol type.

For example, Ångström coefficients < 0.5 would represent the marine domain or the marine aerosol type (see Figures 15a, 15b and 15c). The aerosol components would be any sea-salts with a small admixture of anthropogenic salts like WS2 or WS4. It is possible that a small admixture of OC or BC would also be present. In each case, the mixture giving the best fit would be selected. Similarly, Ångström coefficients between 0.5 and 1.0 would represent the transition state from the marine to the continental domain – the mixed marine-continental aerosol type. Finally,

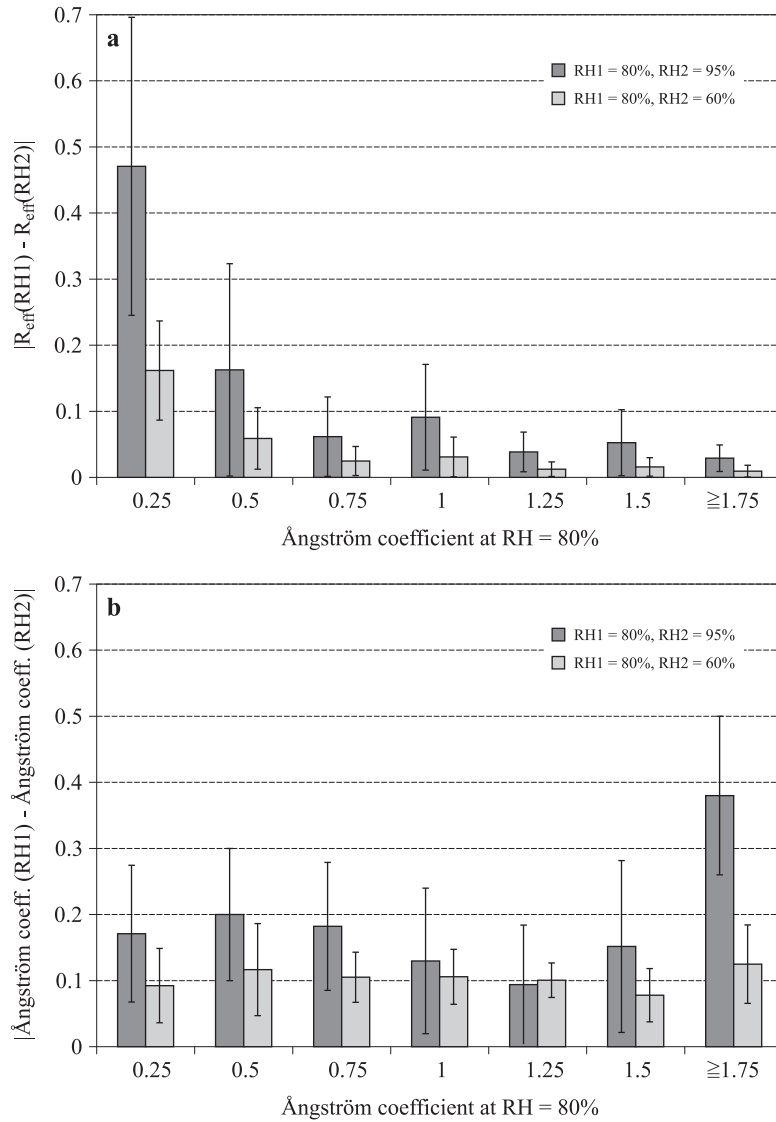


Figure 14. The change in effective radius and Ångström coefficients during the transition from drier to wetter conditions and vice versa. The simulations were done for various mixtures, but the difference is always calculated for the same type of mixture. a) The absolute difference between two values of the effective radius estimated for the same mixture but at different relative humidities (RH), b) The absolute difference between the Ångström coefficients at RH = 80% and RH = 60%, and RH = 80% and RH = 95%

values between 1.0 and 1.5 would indicate the continental aerosol type, and values > 1.5 the industrial aerosol type.

As demonstrated in Figures 15a–15c the general relationship between R_{eff} and the Ångström coefficient for different RHs is very similar. In this sense the classification based on ‘domains’ is independent of RH and therefore very practical: it can be applied as a first guess in aerosol retrieval algorithms, regardless of the ambient RH. A classification of this kind has already been applied successfully by the author, for example to work with GOME remote sensing data (Kuśmierczyk-Michulec & de Leeuw 2005) or to interpret sun photometer data (e.g. Kuśmierczyk-Michulec & Marks 2000).

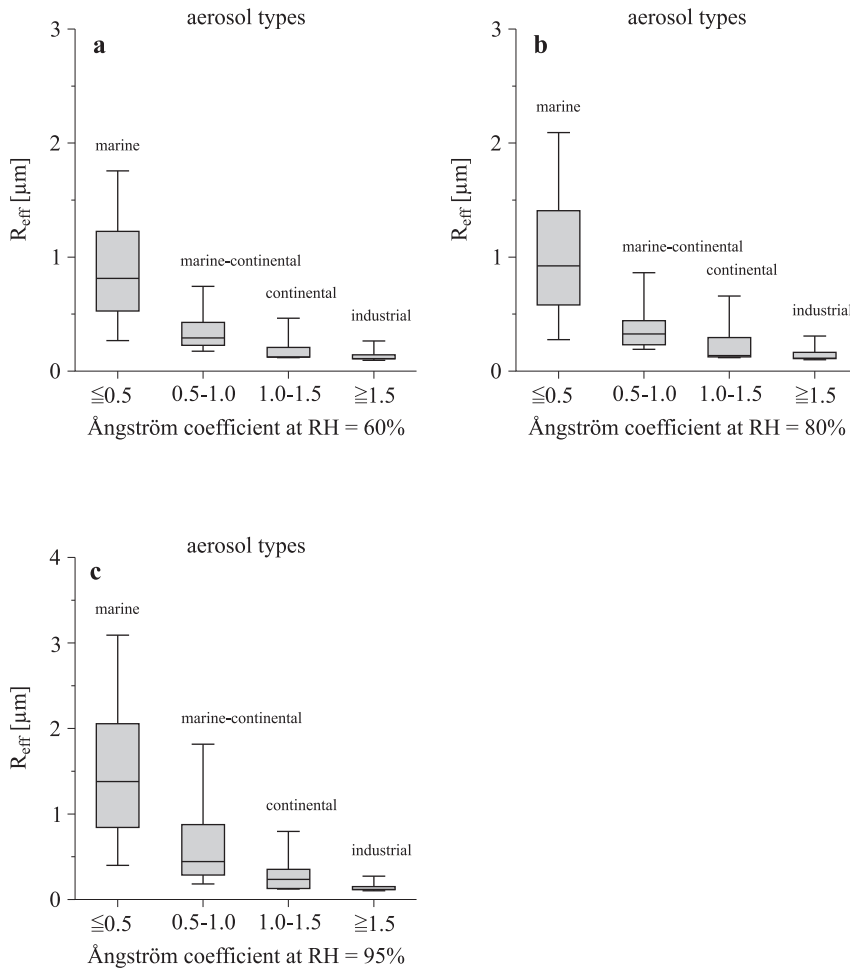


Figure 15. Aerosol types defined in terms of the Ångström coefficient for different relative humidities (RH): a) RH = 60%, b) RH = 80%, c) RH = 95%. An increase in RH causes an increase in R_{eff} , but the general pattern (i.e. the exponential decrease of R_{eff} with increasing Ångström coefficient) is preserved. In this sense the classification based on ‘domains’ is independent of RH

6. Conclusions

This paper investigates the influence of relative humidity on the optical properties of atmospheric aerosol mixtures. The principal conclusions are:

- 1) Relative humidity (RH) modifies the optical properties not only of hygroscopic aerosol mixtures but also of mixtures containing non-hygroscopic aerosols like organic carbon or black carbon. As a result of wetting the hydroscopic particles grow, thereby changing the effective radius of an aerosol mixture and subsequently the aerosol extinction or aerosol optical thickness.
- 2) The observed variations in Ångström coefficients can be explained by changes in the effective radius of a mixture resulting from changes in RH and/or aerosol composition: the larger the number of small aerosol particles, the smaller the effective radius and the larger the Ångström coefficient. However, the change in Ångström coefficient due to variation in RH is far less than that caused by differences in aerosol mixture composition.
- 3) The behaviour of black carbon differed from that of all the other aerosol components considered. The addition of black carbon does not change the effective radius of a mixture but does change the Ångström coefficient. This observation can be explained by its strong absorbing properties of BC, which affect extinction and hence the Ångström coefficient.
- 4) The effective radius (R_{eff}) and Ångström coefficients will change during a transition from drier to wetter conditions or vice versa. This effect is more significant for mixtures with $\alpha \leq 0.5$. The maximum absolute difference between Ångström coefficients calculated at RH = 80% and RH = 60% does not exceed 0.2. The transition from RH = 80% to RH = 95% brings about more significant changes, however. For $\alpha < 1.75$, maximum values do not exceed 0.3, but for $\alpha \geq 1.75$ the maximum absolute difference can be as high as 0.5.
- 5) The Ångström coefficient can be used to define ‘domains’ indicating possible aerosol mixtures and hence the aerosol type. Ångström coefficients < 0.5 would represent the marine domain or marine aerosol type. Values between 0.5 and 1.0 would represent the transition state from the marine to the continental domain – the mixed marine-continental aerosol type; values between 1.0 and 1.5 would be indicative of the continental aerosol type, and $\alpha > 1.5$ would suggest the industrial aerosol type. This kind of domain classification can be applied as a first guess in aerosol retrieval algorithms, regardless of ambient RH.

- 6) An increase in RH causes the effective radius (R_{eff}) to increase; the general pattern (i.e. the exponential decrease in R_{eff} with increase in Ångström coefficient) is preserved, however. In this sense the classification based on ‘domains’ is independent of RH.

Acknowledgements

The author would like to thank all the researchers involved in collecting aerosol data and carrying out the radiosonde measurements during the BASYS Atmospheric Load Experiments. These experiments were supported by the European Community, under EU contracts MAS3-CT96-0058 and IC96-0080 (BASYS/INCO).

References

- Ackerman T.P., Toon O.B., 1981, *Absorption of visible radiation in atmosphere containing mixtures of absorbing and nonabsorbing particles*, Appl. Opt., 20(20), 3661–3668.
- Ångström A., 1929, *On the atmospheric transmission of sun radiation and on dust in the air*, Geogr. Ann., 11, 156–166.
- Berner A., Sidla S., Galambos Z., Kruisz C., Hitzenberg R., ten Brink H.M., Kos G.P.A., 1996, *Modal character of atmospheric black carbon size distributions*, J. Geophys. Res., 101 (D14), 19559–19565.
- Bohren C.F., Huffman D.R., 1983, *Absorption and scattering of light by small particles*, John Wiley, New York, 550 pp.
- Chylek P., Ramaswamy V., Cheng R., Pinnick R.G., 1981, *Optical properties and mass concentration of carbonaceous smokes*, Appl. Opt., 20(17), 2980–2984.
- Gong S.L., Barrie L.A., Blanchet J.-P., 1997, *Modeling sea-salt aerosols in the atmosphere 1. Model development*, J. Geophys. Res., 102 (D3), 3805–3818.
- Heintzenberg J., 1982, *Size segregated measurements of particulate elemental carbon and aerosol light absorption at remote Arctic locations*, Atmos. Environ., 16(10), 2461–2469.
- Hess M., Koepke P., Schultz I., 1998, *Optical properties of aerosols and clouds: The software package OPAC*, Bull. Am. Meteorol. Soc., 79(5), 831–844.
- IPCC – Intergovernmental Panel on Climate Change, 2007, *The physical science basis, Contribution of Working Group I to the Fourth Assessment Report*, (available at <http://www.ipcc.ch/ipccreports/ar4-syr.htm>).
- Kanakidou M., Seinfeld J.H., Pandis S.N. et al., 2005, *Organic aerosol and global climate modelling: a review*, Atmos. Chem. Phys., 5(4), 1053–1123.
- Kuśmierczyk-Michulec J., van Eijk A.M.J., 2007, *Ångström coefficient as a tracer of the continental aerosols*, Proc. SPIE, 6708–25, Atmospheric Optics: Models, Measurements, and Target-in-the-Loop Propagation, 27–28 August 2007, San Diego, CA.

- Kuśmierczyk-Michulec J., de Leeuw G., 2005, *Aerosol optical thickness retrieval over land and water using Global Ozone Monitoring Experiment (GOME) data*, J. Geophys. Res., 110, D10S05, doi:10.1029/2004JD004780.
- Kuśmierczyk-Michulec J., de Leeuw G., Robles Gonzalez C., 2002, *Empirical relationships between aerosol mass concentrations and Ångström parameter*, Geophys. Res. Lett., 29 (7), 1145, doi:10.1029/2001GL014128.
- Kuśmierczyk-Michulec J., Marks R., 2000, *The influence of sea-salt aerosols on the atmospheric extinction over the Baltic and the North Seas*, J. Aerosol Sci., 31 (11), 1299–1316.
- Kuśmierczyk-Michulec J., Schulz M., Ruellan S., Krüger O., Plate E., Marks R., de Leeuw G., Cachier H., 2001, *Aerosol composition and related optical properties in the marine boundary layer over the Baltic Sea*, J. Aerosol Sci., 32 (8), 933–955.
- McClatchey R. A., Bolle H.-J., Kondratyev K. Y., Joseph J. H., McCormick M. P., Raschke E., Pollack J. B., Spänkuch D., Mateer C., 1984, *A preliminary cloudless standard atmosphere for radiation computation*, Rep. Int. Radiat. Comm., Boulder, CO, 53 pp.
- Mie G., 1908, *Annales de Physic*, 25, 377–445.
- Olszewski J., Kuśmierczyk-Michulec J., Sokólski M., 1995, *The method of continuous measurement of the diffusivity of the natural light field*, Oceanologia, 37 (2), 299–310.
- Orr Jr. C., Hurd F. K., Corbett W. J., 1958, *Aerosol size and relative humidity*, J. Colloid Sci., 13, 472–482.
- Plate E., 2000, *Variabilität der Zusammensetzung anorganischer Aerosole – insbesondere der reaktiven Stickstoffverbindungen – in küstennahen Gebieten der Nordsee und Ostsee*, Ph.D. thesis, Univ. Hamburg, Germany.
- Richardson C. B., Kurtz C. A., 1984, *A novel isopiestic measurement of water activity in concentrated and supersaturated lithium halide solutions*, J. Am. Chem. Soc., 106 (22), 6615–6618.
- Richardson C. B., Spann J. F., 1984, *Measurement of the water cycle in a levitated ammonium sulfate particle*, J. Aerosol Sci., 15, 563–571.
- Rulleau S., 2000, *Comparative study of carbonaceous aerosol in tropical, urban and arctic atmospheres: specificity of sources and atmospheric evolution*, Ph.D. thesis, LSCE, CEA/CNRS, Gif-Sur-Yvette, Cedex, France, (in French).
- Schulz M., Cachier H., Ebinghaus R., Ferm M., Hongisto M., Iverfeldt A., Jylha A., Krueger O., Kuśmierczyk-Michulec J., de Leeuw G., Marks R., Moermann M., Munthe J., Nadstazik A., Ruellan S., Petersen G., Plate E., Ulevicius V., Schneider B., Schmolke S., Sopauskiene D., 1999, *Evolution of the aerosol composition in the BASYS network study and Lagrangian experiments in summer 1997 and winter 1998*, J. Aerosol Sci., 30, Suppl. 1, 97–98.
- Sinfeld J. H., Pandis S. N., 1998, *Atmospheric chemistry and physics: from air pollution to climate change*, John Wiley and Sons, New York, 1326 pp.

-
- Shettle E. P., Fenn R. W., 1979, *Models of aerosols of lower troposphere and the effect of humidity variations on their optical properties*, AFCRL Tech. Rep. 79 0214, Air Force Cambridge Res. Lab., Hanscom Air Force Base, MA, 10 pp.
- Sloane C. S., 1983, *Optical properties of aerosols – comparison of measurements with model calculations*, Atmos. Environ., 17 (2), 409–416.
- Stier P., Feichter J., Kinne S., Kloster S., Vignati E., Wilson J., Ganzeveld L., Tegen I., Werner M., Balkanski Y., Schulz M., Boucher O., Minikin A., Petzold A., 2005, *The aerosol-climate model ECHAM5-HAM*, Atmos. Chem. Phys., 5 (4), 1125–1156, [<http://www.atmos-chem-phys.org/acp/5/1125>].
- Tang I. N., 1976, *Phase transformation and growth of aerosol particles composed of mixed salts*, J. Aerosol Sci., 7, 361–371.
- Tang I. N., 1996, *Chemical and size effects of hygroscopic aerosols on light scattering coefficients*, J. Geophys. Res., 101 (D14), 19245–19250.
- Tang I. N., 1997, *Thermodynamic and optical properties of mixed-salt aerosols of atmospheric importance*, J. Geophys. Res., 102 (D2), 1883–1893.
- Tang I. N., Munkelwitz H. R., 1984, *An investigation of solute nucleation in levitated solution droplets*, J. Colloid Interf. Sci., 98 (2), 430–438.
- Tang I. N., Munkelwitz H. R., 1994, *Water activities, densities, and refractive indices of aqueous sulfates and sodium nitrate droplets of atmospheric importance*, J. Geophys. Res., 99 (D9), 18801–18808.

Appendix 1

External mixing approach

The aerosol optical thickness τ_a depends on the contribution of all aerosol components in a given aerosol mixture and can be written as:

$$\tau_a(\lambda, RH) = \sum_{j=1}^4 C_{V,tot}^j(RH) \times \frac{ext^j(\lambda, RH)}{C_V^j(RH)} = \sum_{j=1}^4 C_{V,tot}^j(RH) \times \psi^j(\lambda, RH), \quad (A1-1)$$

where the index $j = 1, \dots, 4$ symbolises the aerosol components SSA, WS, OC and BC. ψ^j indicates the aerosol extinction of the j^{th} component with respect to its volume concentration $C_V^j [\mu\text{m}^3 \text{cm}^{-3}]$ and $C_{V,tot}^j [\mu\text{m}^3 \mu\text{m}^{-2}]$ is the total volume of the j^{th} aerosol component in the whole column of the atmosphere. The above equation can be rewritten in terms of one component, e.g. SSA, and indicated as $j = 1$.

$$\tau_a(\lambda, RH) = C_{V,tot}^1(RH) \left\{ \psi^1(\lambda, RH) + \sum_{j=2}^4 \frac{C_{V,tot}^j(RH)}{C_{V,tot}^1(RH)} \psi^j(\lambda, RH) \right\}. \quad (A1-2)$$

For a given wavelength, e.g. $\lambda_1 = 555 \text{ nm}$ and ambient relative humidity, e.g. RH_{meas} , equation (A1-2) can be written as

$$\begin{aligned} \tau_a(\lambda_1, RH_{meas}) = & C_{V,tot}^1(RH_{meas}) \left\{ \psi^1(\lambda_1, RH_{meas}) + \right. \\ & \left. + \sum_{j=2}^4 \frac{C_{V,tot}^j(RH_{meas})}{C_{V,tot}^1(RH_{meas})} \psi^j(\lambda_1, RH_{meas}) \right\}. \end{aligned} \quad (A1-3)$$

The relation between $C_{V,tot}^j(RH_{meas})$ and the total volume of all aerosols in the whole column $C_{V,tot}(RH_{meas})$ can be expressed in the following way:

$$C_{V,tot}^j(RH_{meas}) = \chi_j C_{V,tot}(RH_{meas}), \quad (A1-4)$$

where χ_j satisfies the condition

$$\sum_{j=1}^4 \chi_j = 100\%. \quad (A1-5)$$

Equations (A1-4) and (A1-5) lead to the relation

$$\sum_{j=1}^4 C_{V,tot}^j(RH_{meas}) = C_{V,tot}(RH_{meas}) \sum_{j=1}^4 \chi_j = C_{V,tot}(RH_{meas}). \quad (A1-6)$$

Assuming that $\tau_a(\lambda_1, RH_{meas})$ and χ_j are known, and using equations (A1–2) to (A1–6), the parameter $C_{V,tot}^1(RH_{meas})$ can be calculated as follows:

$$C_{V,tot}^1(RH_{meas}) = \tau_a(\lambda_1, RH_{meas}) \left\{ \sum_{j=1}^4 \frac{\chi_j}{\chi_1} \psi^j(\lambda_1, RH_{meas}) \right\}^{-1}. \quad (\text{A1-7})$$

The general relation between the volume concentration and the number concentration is given by equation (4) (see section 2.1). Thus, knowing $C_{V,tot}^1(RH_{meas})$ it is possible to calculate $N_{n,tot}^1$ i.e. the number concentration of the first aerosol component (in the whole column). The other $N_{n,tot}^j$ parameters for the remaining components can be obtained in a similar way. Since $N_{n,tot}^j$ does not depend on RH, these numbers will be used to estimate $C_{V,tot}^j(RH)$ for any RH value.

Appendix 2

Formula for the Ångström coefficient as a function of relative humidity for a three-component aerosol mixture

The Ångström coefficient for a mixture of SSA and two other components, e.g. WS and OC, is

$$\begin{aligned} \alpha_{mix}(RH) = \alpha^{SSA}(RH) - \frac{1}{\ln\left(\frac{\lambda_1}{\lambda_2}\right)} & \left\{ \ln \left[1 + \frac{y^{WS}}{\xi_1} \left(\frac{\lambda_1}{\lambda_2}\right)^{-\alpha^{mix1}} + \right. \right. \\ & \left. \left. + \xi_2 \frac{y^{OC}}{\xi_1} \left(\frac{\lambda_1}{\lambda_2}\right)^{-\alpha^{mix2}} \right] - \ln \left(1 + \frac{y^{WS}}{\xi_1} + \xi_2 \frac{y^{OC}}{\xi_1} \right) \right\}. \quad (\text{A2-1}) \end{aligned}$$

The parameter y^{WS} is defined as the ratio of ψ^{WS} to ψ^{SSA}

$$y^{WS} = \frac{\psi^{WS}(\lambda_2, RH)}{\psi^{SSA}(\lambda_2, RH)}. \quad (\text{A2-2})$$

Similarly, y^{OC} is defined as the ratio of ψ^{OC} to ψ^{SSA}

$$y^{OC} = \frac{\psi^{OC}(\lambda_2)}{\psi^{SSA}(\lambda_2, RH)}. \quad (\text{A2-3})$$

The coefficient α^{mix1} is the difference between α^{WS} and α^{SSA}

$$\alpha^{mix1} = \alpha^{WS} - \alpha^{SSA}. \quad (\text{A2-4})$$

Analogously, the coefficient α^{mix2} is expressed in terms of α^{OC} and α^{SSA}

$$\alpha^{mix2} = \alpha^{OC} - \alpha^{SSA}. \quad (\text{A2-5})$$

The parameter ξ_1 is defined as the ratio of χ^{SSA} to χ^{WS} :

$$\xi_1 = \frac{\chi^{SSA}}{\chi^{WS}} = \frac{100 - \chi^{WS} - \chi^{OC}}{\chi^{WS}}. \quad (\text{A2-6})$$

In a similar way, ξ_2 relates χ^{OC} to χ^{WS} :

$$\xi_2 = \frac{\chi^{OC}}{\chi^{WS}}. \quad (\text{A2-6})$$